Metallic Spiral Three-Dimensional Photonic Crystal with a Full Band Gap at Optical Communication Wavelengths
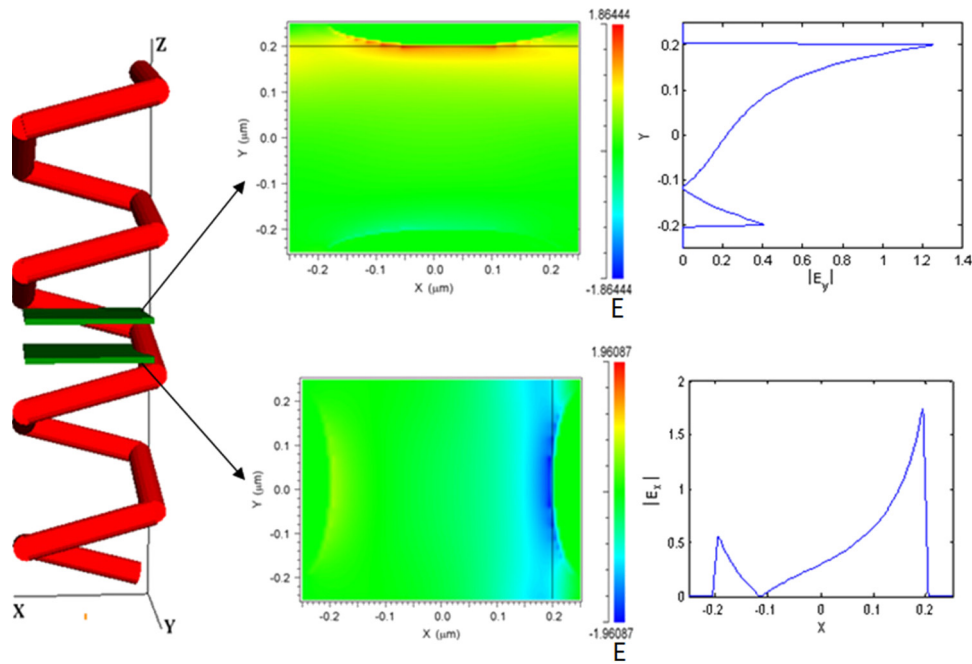
Po Sun
John D. Williams

Metallic Spiral Three-Dimensional Photonic Crystal with a Full Band Gap at Optical Communication Wavelengths

Po Sun and John D. Williams

University of Alabama in Huntsville, Department of Electrical and Computer Engineering,
Huntsville, AL 35899 USA

Abstract: The optical properties of a gold spiral photonic crystal (PC) were studied numerically and a full 3-D band gap at near infrared wavelengths was found. This band gap, ranging from 1.2 to 1.8 μm in wavelength, covers all the second and third telecom windows used in optical fiber communications. Chiral and other optical properties were also discussed. There is a very high absorption at the band gap edge due to the retarded speed of light and an abnormal high transmission outside the band gap contributed by surface plasmon polaritons. Both right circular polarized (RCP) and left circular polarized (LCP) light are studied and great diversities were found in certain regions of the spectrum. These optical properties maintain within large incident angles.

Index Terms: Photonic crystals, photonic band gap structures, plasmonics.

1. Introduction

Three-dimensional metallic photonic crystals (PCs) are used for a number of applications such as thermophotovoltaics and regulation of blackbody emissions [1], [2]. However, it is much harder to study metallic PCs than their dielectric counterparts due to the large dispersive and absorbing property of metals. For example, it is still a challenging task to calculate the full band structure of a 3-D metallic PC. Among 3-D metallic PCs, the woodpile structure has obtained the most attention and has been fabricated using multiple metals [2]–[4]. To prove the existence of the photonic band gap, researchers have to measure the reflectance spectrum of woodpiles in a wide solid angle range either experimentally [2], [3] or through simulation [4].

Spiral structures made of dielectric material were theoretically proven to be promising 3-D photonic-band-gap structures with sizable band gaps by Chutinan and Noda [5]. Toader and John proposed a spiral PC of tetragonal lattice made of silicon which has a band gap between the fourth and fifth bands [6], [7]. Much of published research later focused on fabrication and band gap studies of the spiral 3-D PC made of silicon or dielectric materials [8]–[13]. However, these studies cannot come to a foregone conclusion that spiral structures made of metals would also demonstrate a full 3-D band gap, since the light is mostly reflected with loss in metal structures while refracted in dielectric structures [14]. Other efforts studied the metallic spiral structure as a circular polarizer based on the different polarization optical properties of helix handedness [15]–[17]. Due to the difficulties discussed above, a full 3-D band gap has never been found in metallic spiral structures. In this article, the full band structure of a metallic 3-D spiral PC is obtained and a full 3-D band gap
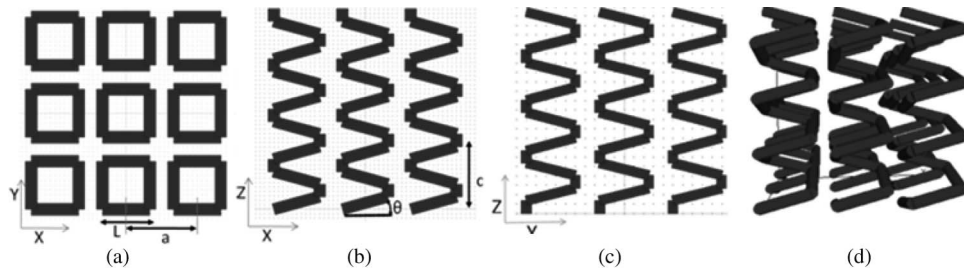
Fig. 1. Schematics of the spiral photonic crystal in different perspective views (a)–(c) and the 3-D view (d).
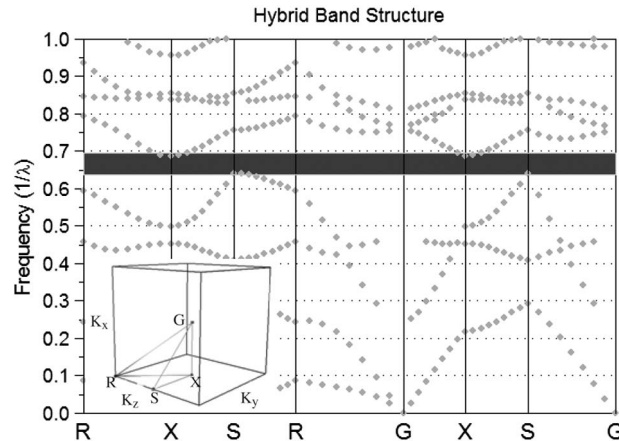

Fig. 2. Band structure of the gold spiral 3-D photonic crystal. The subgraph shows the first Brillouin zone and the K path; frequency is normalized to λ, the wavelength in the free space.

for this structure is found. This article also presents multiple optical properties exclusive to this metallic PC such as chiral symmetry, abnormally high absorptions and high transmissions.

2. Structure of the Spiral PC

The 3-D PC structure consists of cylindrical gold posts which spiral squarely. These spirals are then arranged on a 2-D square lattice, making a 3-D tetragonal lattice. Fig. 1 shows this structure from different perspectives and depicts the geometric parameters. The PC has periods a along x- and y-directions and c along the z-direction; the rising angle of the posts is θ, and the length and radius of the posts are represented by $L/\cos(\theta)$ and R, respectively. The parameters L, c, and θ have relation of $\tan(\theta) = c/4L$. Therefore, the primitive lattice vectors of this tetragonal lattice are $(a, 0, 0)$, $(0, a, 0)$, and $(0, 0, c)$ and the unit cell is one spiral space $(a \times a \times c)$.

3. Results and Analysis

A popular way to obtain band structures of PCs is to solve frequency domain eigenproblems with the plane wave expansion method [18], [19]. The loss and dispersive properties of gold make direct calculation of the band structure using this technique more difficult. For this effort, the commercial software package, R-soft, was used to calculate the band structure with a finite-difference time-domain method (FDTD). In the FDTD approach, periodic boundary conditions are set and an impulse source (broad spatial frequencies) is launched to activate broad temporal frequencies. The spectral response is then obtained by Fourier Transform analysis. The eigenfrequencies of each band can be determined from the peaks of the response spectrum. The complex permittivity of the metal was calculated from the Lorentz–Drude model [20]. Fig. 2 shows the band structure of a gold spiral 3-D PC where $a = L$, $\theta = 15°$, $R = L/5$, and $L = 0.5\ \mu$m. A 3-D band gap opens between the
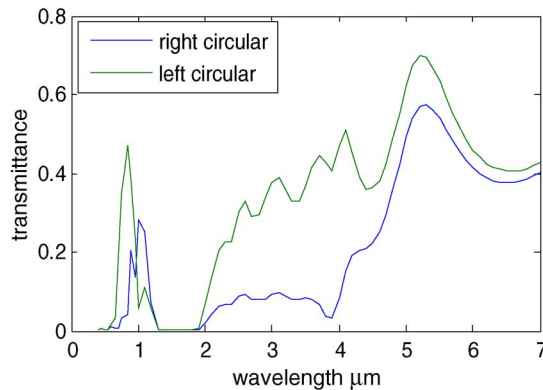
Fig. 3. Normal incidence (along *z*-direction) transmittance of the gold spiral photonic crystal for both right and left circular polarization.
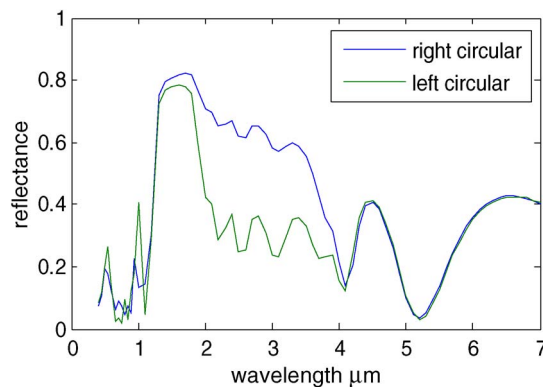

Fig. 4. Normal incidence (along *z*-direction) reflectance of the gold spiral photonic crystal for both right and left circular polarization.

fourth and fifth bands, similar in nature to that calculated for a dielectric spiral 3-D PC [5]–[7]. The frequency in Fig. 2 is normalized to the wavelength in free space, λ, so the forbidden spectrum (band gap) is centered about at $\lambda = 1/0.67 = 1.5$ μm.

To confirm the existence of the 3-D band gap and make a further study of this structure, the optical propagation of the electromagnetic wave along the *z*-direction was simulated with the FDTD method. Figs. 3–5 show the transmittance, reflectance and absorptance spectra of the gold spiral PC, which has a four-period height along *z*-direction. As shown in Fig. 1(d), the structure is a right-handed spiral if the light is launched from the bottom. Likewise, two oppositely handed circular polarized light waves [right circular polarized (RCP) and left circular polarized (LCP)] were defined and simulated, respectively. From the transmittance and reflectance, a clearly forbidden spectrum for both RCP and LCP light from 1.2 μm to 1.8 μm can be found, which exactly fits the full 3-D band gap in Fig. 2. So both the band structure and the propagation spectra demonstrate the existence of the 3-D band gap.

Meanwhile, a series of simulations with different incident angles were performed to this structure. Fig. 6(a) and (b) show the simulating transmittance with different tilted angles for both LCP and RCP light, where the angles of direction (Θ, Φ) are shown in the subplots. Due to the symmetry of the structure, tilting angles along x and *y*-direction (i.e., $\Phi = 0°$ and $\Phi = 90°$) has same effect, so only the cases $\Phi = 0°$ and $45°$ were simulated. All these results demonstrate the full band gap from 1.2 μm to 1.8 μm. For the case Θ and Φ equal $45°$, there is a partial band gap from 2.2 μm to 4 μm, where the transmittance of both right and left circular wave become zero. Notice that the significant
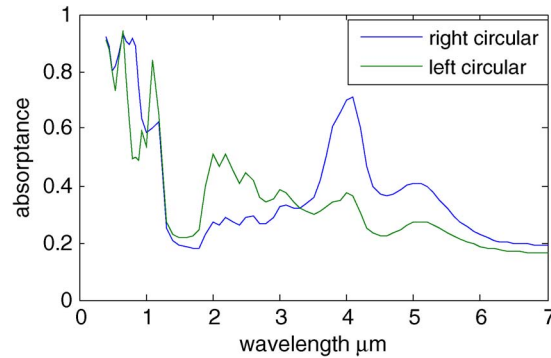
Fig. 5. Normal incidence (along *z*-direction) absorptance of the gold spiral photonic crystal for both right and left circular polarization.
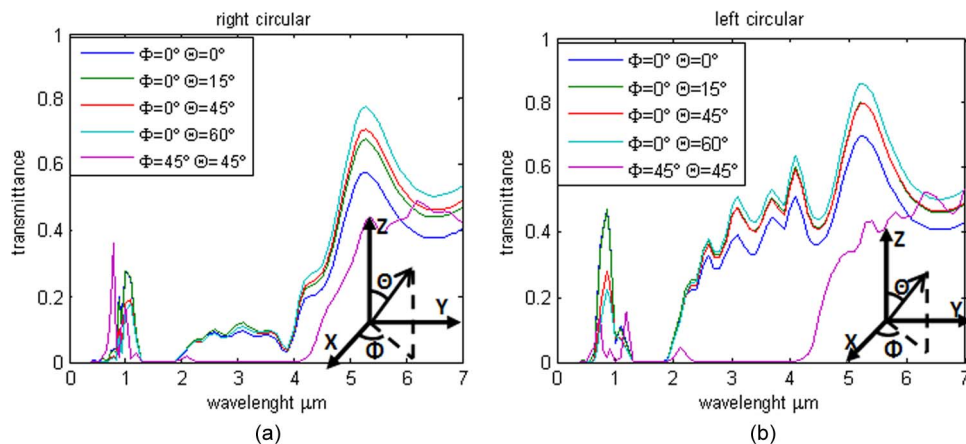

Fig. 6. Transmittance of the gold spiral photonic crystal for (a) right and (b) left circular polarization with different incident angles.

difference between LCP and RCP propagation (chiral property) happens to be in this wave length range (2.2 μm $\sim$ 4 μm), while the existence of this partial band gap makes the difference disappear for the incident angle $\Theta = \Phi = 45°$.

In addition to a full band gap, this structure also has very interesting optical characteristics. An absorptance peak over 0.8 for LCP and 0.6 for RCP light shows up at 1.2 μm, as shown in Fig. 5, which is the band gap edge of the PC. This phenomenon can also be found in other metallic 3-D PCs due to the retarded speed and the percolation effects of light near the photonic band gap edge [2]. Beyond the band gap $(\lambda > 2\ \mu$m), the transmittance and reflectance oscillate and noticeably high transmittance peaks appear. Fig. 6 shows a transmittance peak at 5.2 μm both for LCP and RCP light. To better explain this phenomenon, one needs to review the structure schematics again. Fig. 1(a) is the view from the bottom side and the simulated lights were launched in this direction with different inclined angles. For the simulated structure, (the parallel period) *a* equals (the projected length) *L* of the posts, i.e., $a = L$. This makes the edges of the spirals overlap each other (or there is no space between spirals) from this direction. Therefore, from this perspective, it is like a gold film with square holes arranged on a 2-D square lattice. Note that the size of the holes (0.5 μm) is much smaller than the wave length (5.2 μm), so the transmission modes cannot be explained by a simple wave guide. Similar extraordinary optical transmission was also observed in the subwavelength hole arrays in metallic films and attributed to the surface plasmons [21]–[25]. Surface plasmons were also proven to contribute to the passband modes in 3-D complex metallic structures [4]. The abnormally high transmission in this case can also be explained by the surface plasmon
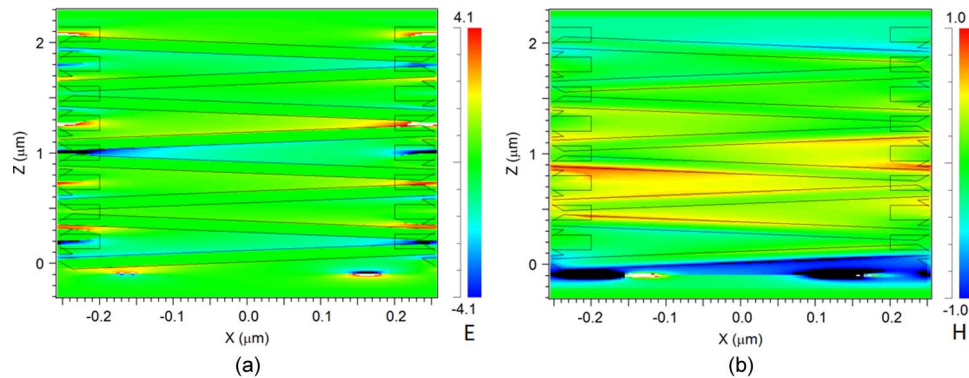
Fig. 7. (a) Electric field and (b) Magnetic field contour for the *x–z* section of the gold spiral photonic crystals.
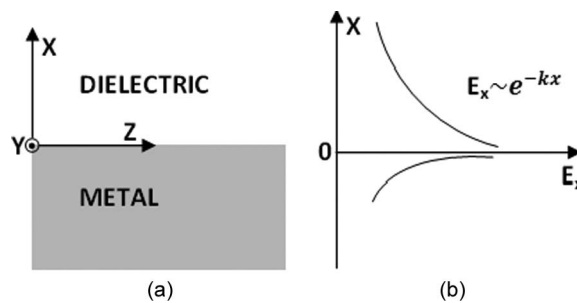

Fig. 8. (a) Geometry of the surface plasmon polaritons propagation at a single interface and (b) the exponential dependence of Ex fields.

excitation. Fig. 7(a) and (b) show the light of wavelength $\lambda = 5.2~\mu$m propagation in the x-z cross section, where the electric field [E, in Fig. 7(a)] and Magnetic field [H, in Fig. 7(b)] are represented by colors and the dark lines outline the boundary of the structure. Both E and H are normalized to the launched source light. Fig. 7 shows that the electromagnetic field is primarily distributed on the boundary of the structure and that the electric field resonance conditions are much larger than the source field. This is the same phenomenon as the typical surface plasmon effect. It is important to notice that the field resonance is extremely large on the edges of the lattice unit, where the spirals interlace. This indicates that the interaction between spirals contributes greatly to light propagation. Therefore, changing the distance between spirals, *a*, will significantly change the light propagation in the structure. To see the influence of period (a) on the light propagation, band structures of the PCs with different periods are calculated. The results show that the band gap is maximized when $a = L$ and will disappear if *a* is greater than 1.1 *L* or less than 0.9 *L*. Therefore, to get a full band gap, only a small range of the period can be chosen.

To study the surface plasmon effect in this structure, it is useful to take a look at the surface plasmon polaritons at a single interface. Fig. 8(a) shows the geometry of an interface between a metal and a dielectric assuming the surface plasmon polaritons propagate along *z*-direction. For transverse magnetic (TM) modes, the magnetic fields (H) are along *y*-direction (i.e., tangent to the interface) and electric fields (E) are along *x*-direction (vertical to the interface); for transverse electric (TE) modes, E fields are tangent to the interface and H fields vertical to the interface. The surface plasmon polaritons are proven to have two unique characters [26], [27]: 1) surface plasmon polaritons only exist for TM polarization, i.e., E fields are vertical to the interface; and 2) Electromagnetic fields maximize at the interface and decay exponentially away from the
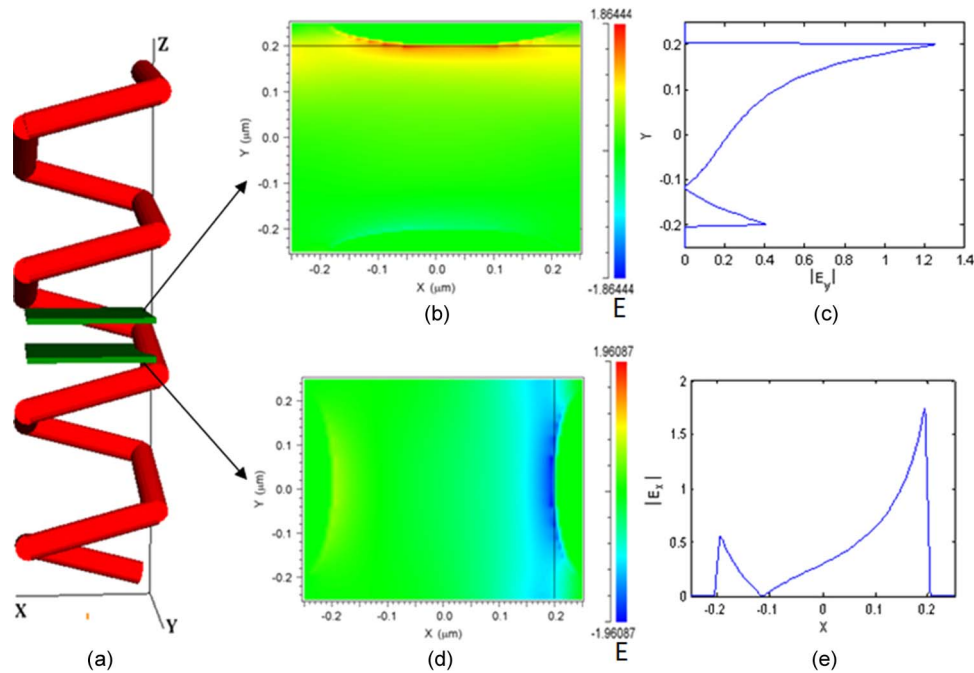
Fig. 9. (a) Two x–y cross sections (green surfaces) in one spiral cut at different position along z-direction: (b) Ey field contour on the cross section where the interface is along x-direction; (c) 1-D slice profile of Ey in (b) when $x = 0$; (d) Ex field contour on the cross section where the interface is along y-direction; (e) 1-D slice profile of Ex in (d) when $y = 0$.

interface. In Fig. 8, the interface is located at $x = 0$ and the exponential dependence of E fields is shown in Fig. 8(b).

In the spiral structure, the extraordinary transmission is primarily due to the TM mode surface plasmon polaritons. To demonstrate this phenomenon, a circular polarization light with wavelength $\lambda = 5.2~\mu$m is launched from the bottom of the structure, which can excite the polarization mode along any direction. The following study, however, will show that only the TM surface plasmon polaritons can be significantly watched in the structure. It is not exactly proper to say TM mode or TE mode here, since the structure is 3-D. Here, the TM mode refers to the polarization mode that the E field is vertical to the interface between a metal and a dielectric and TE mode means E field is parallel to the interface. If x–y cross sections are cut at different z position, different profiles will be seen. Fig. 9(a) shows one spiral and two cross sections (green surfaces) cut at different z positions. The two cross sections intersect two different gold logs, respectively, so the interfaces between the metal and the dielectric are located in different positions in the two cross sections. For the upper cross section, the interface is along x-direction. In Fig. 9(b), the dark line represents the interface: Metal is upper side of this line and dielectric below of this line. For the below cross section [Fig. 9(d)], the interface is along y-direction: the left side is dielectric and the right side is metal. Fig. 9(b) is the Ey contour of the upper cross section and Fig. 9(d) is the Ex contour of the below cross section, where the color represents the amplitude of Ey or Ex. Here, Ex represents the electric field along x-direction and Ey along y-direction. One can see that E field is mainly distributed near the interfaces between metals and dielectrics where the polarization of the E field is vertical to the interface, as in Fig. 9(b) and (d). Fig. 9(c) and (e) are 1-D slice profiles of Fig. 9(b) and (d), where $x = 0$ [for Fig. 9(c)] or $y = 0$ [for Fig. 9(e)]. Fig. 9(c) is a y-versus-Ey plot while Fig. 9(e) x-versus-Ex. Here, absolute values of Ey and Ex are used and the Ey is put on the parallel axis while Ex is put on the vertical axis in order to compare the 2-D contour left to them. From these two plots one can see that the E field maximize at the interface and decay exponentially away from the interface, just like in Fig. 8(b). There is another peak on the other side. This is due to the gold log from the neighbor spiral which is just located at that position, although it is not shown in the Fig. 9(a).
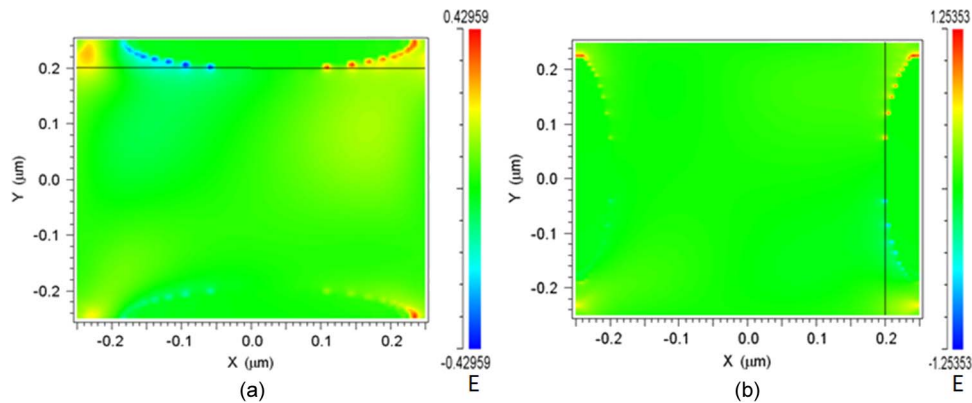
Fig. 10. Electric field contour on the *x−y* cross sections of the gold spiral photonic crystal: (a) Ex, the interface is along *x*-direction; (b) Ey, the interface is along *y*-direction.
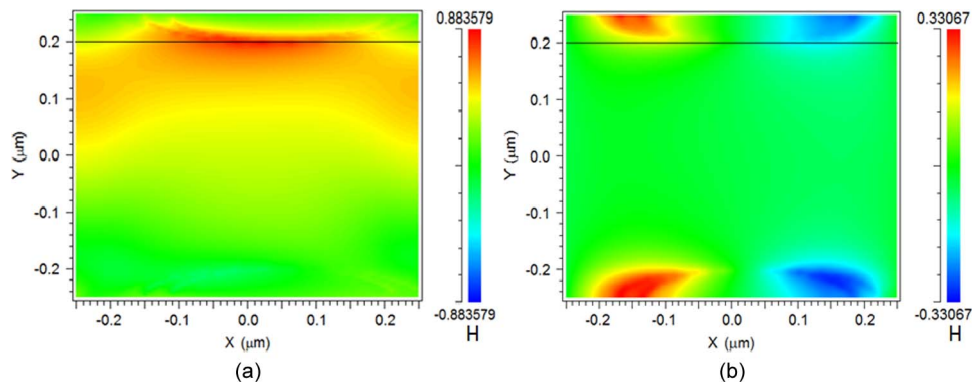

Fig. 11. Magnetic field contour on the *x−y* cross section where the interface is along *x*-direction: (a) Hx, the field along *x*-direction, which is parallel to the interface and (b) Hy, the field along *y*-direction, which is vertical to the interface.

When E field is parallel to the interface, the propagation mode does not exist (or very weak) as shown in Fig. 10(a) and (b), which is the E field contour where the polarization is parallel to the interface [Ex for Fig. 10(a) and Ey for Fig. 10(b)]. Although strong fields are found at corners, this is because the gold posts in other spirals interlace at the corners and contribute to the surface plasmon polaritons. The point-like distribution of the electric field in Fig. 10 is due to the round surface of the post near the cross section, which excites some weak electric fields.

Likewise, the TM mode surface plasmon polaritons can be demonstrated also by watching magnetic field distribution. Fig. 11(a) and (b) show the magnetic fields with different polarization Hx (*x*-direction) and Hy (*y*-direction) on the same *x−y* cross section as in Fig. 9(b), where the interface is along *x*-direction. A similar phenomenon can be found in these figures except that the H field tangent to the interface represents the TM mode, which is opposite to the E field.

Another unique optical characteristic of the spiral PC is the chiral performance for different handed circular polarized light wavelengths. This has led to the investigation of polarization gaps [11] and the design of circular polarizers with them [15]. The metallic spiral structure presented in this letter also exhibits this circular polarization characteristic. Figs. 3 and 4 show significantly different propagation characteristics between LCP and RCP light between 2 μm to 4 μm. These spectra can be seen as a partial polarization band gap exclusive to RCP light. The absorptance peak for RCP light at 4 μm (Fig. 5) can also be explained by the retarded speed and percolation effects of light at the band gap edge.

4. Conclusion

A gold spiral 3-D PC was studied numerically. The band structure was calculated and a full 3-D band gap centered at 1.5 μm was obtained. Surface plasmon effect in this PC was studied and proven to contribute to the transmission beyond the cutoff wavelength. Other special optical features were also discussed. There is an abnormal high absorption at the band gap edge due to the retarded speed of light, and the chiral optical property was also found in certain spectrum. These features were found to be available in large incident angles for this spiral metallic PC.

References

[1] E. Yablonovitch, "Inhibited spontaneous emission in solid-state physics and electronics," *Phys. Rev. Lett.*, vol. 58, no. 20, pp. 2059–2062, May 1987.

[2] J. Fleming, S. Lin, I. El-Kady, R. Biswas, and K. Ho, "All-metallic three-dimensional photonic crystals with a large infrared bandgap," *Nature*, vol. 417, no. 6884, pp. 52–55, May 2002.

[3] J. D. Williams, P. Sun, W. C. Sweatt, and A. R. Ellis, "Metallic-tilted woodpile photonic crystals in the midinfrared," *J. Micro/Nanolithography MEMS MOEMS*, vol. 9, no. 2, p. 023011, Apr. 2010.

[4] P. Sun and J. D. Williams, "Passband modes beyond waveguide cutoff in metallic tilted-woodpile photonic crystals," *Opt. Exp.*, vol. 19, no. 18, pp. 7373–7380, Apr. 2011.

[5] A. Chutinan and S. Noda, "Spiral three-dimensional photonic-band-gap structure," *Phys. Rev. B*, vol. 57, no. 4, pp. R2006–R2008, Jan. 1998.

[6] O. Toader and S. John, "Proposed square spiral microfabrication architecture for large three-dimensional photonic band gap crystals," *Science*, vol. 292, no. 5519, pp. 1133–1135, May 2001.

[7] O. Toader and S. John, "Square spiral photonic crystals: Robust architecture for microfabrication of materials with large three-dimensional photonic band gaps," *Phys. Rev. E*, vol. 66, no. 1, p. 016610, Jul. 2002.

[8] S. R. Kennedy, M. J. Brett, O. Toader, and S. John, "Fabrication of tetragonal square spiral photonic crystals," *Nano Lett.*, vol. 2, no. 1, pp. 59–62, 2002.

[9] S. R. Kennedy, M. J. Brett, H. Miguez, O. Toader, and S. John, "Optical properties of a three-dimensional silicon square spiral photonic crystal," *Photon. Nanostruct.—Fundam. Appl.*, vol. 1, no. 1, pp. 37–42, Dec. 2003.

[10] M. Jensen and M. Brett, "Square spiral 3D photonic bandgap crystals at telecommunications frequencies," *Opt. Exp.*, vol. 13, no. 9, pp. 3348–3354, May 2005.

[11] J. Lee and C. Chan, "Polarization gaps in spiral photonic crystals," *Opt. Exp.*, vol. 13, no. 20, pp. 8083–8088, Oct. 2005.

[12] K. Seet, V. Mizeikis, S. Juodkazis, and H. Misawa, "Three-dimensional circular spiral photonic crystal structures recorded by femtosecond pulses," *J. Non-Cryst. Solids*, vol. 352, no. 23–25, pp. 2390–2394, Jul. 2006.

[13] M. Thiel, M. Decker, M. Deubel, M. Wegener, S. Linden, and G. von Freymann, "Polarization stop bands in Chiral polymeric three-dimensional photonic crystals," *Adv. Mater.*, vol. 19, no. 2, pp. 207–210, Jan. 2007.

[14] E. D. Palic, *Handbook of Optical Constants of Solids I, Subpart 1.* New York: Academic, 1998.

[15] J. K. Gansel, M. Thiel, M. S. Rill, M. Decker, K. Bade, V. Saile, G. von Freymann, S. Linden, and M. Wegener, "Gold helix photonic metamaterial as broadband circular polarizer," *Science*, vol. 325, no. 5947, pp. 1513–1515, Sep. 2009.

[16] J. K. Gansel, M. Wegener, S. Burger, and S. Linden, "Gold helix photonic metamaterials: A numerical parameter study," *Opt. Exp.*, vol. 18, no. 2, pp. 1059–1069, Jan. 2010.

[17] Z. Yang, M. Zhao, and P. Lu, "Improving the signal-to-noise ratio for circular polarizers consisting of helical metamaterials," *Opt. Exp.*, vol. 19, no. 5, pp. 4255–4260, Feb. 2011.

[18] S. Shi, C. Chen, and D. W. Prather, "Plane-wave expansion method for calculating band structure of photonic crystal slabs with perfectly matched layers," *J. Opt. Soc. Amer. A*, vol. 21, no. 9, pp. 1769–1775, Sep. 2004.

[19] S. Johnson and J. Joannopoulos, "Block-iterative frequency-domain methods for Maxwell's equations in a planewave basis," *Opt. Exp.*, vol. 8, no. 3, pp. 173–190, Jan. 2001.

[20] A. D. Rakic, A. B. Djurisic, J. M. Elazar, and M. L. Majewski, "Optical properties of metallic films for vertical-cavity optoelectronic devices," *Appl. Opt.*, vol. 37, no. 22, pp. 5271–5283, Aug. 1998.

[21] T. W. Ebbesen, H. J. Lezec, H. F. Ghaemi, T. Thio, and P. A. Wolff, "Extraordinary optical transmission through sub-wavelength hole arrays," *Nature*, vol. 391, no. 6668, pp. 667–669, Feb. 1998.

[22] U. Schroter and D. Heitmann, "Surface-plasmon-enhanced transmission through metallic gratings," *Phys. Rev. B*, vol. 58, no. 23, pp. 15 419–15 421, Dec. 1998.

[23] L. Martin-Moreno, F. J. Garcia-Vidal, H. J. Lezec, K. M. Pellerin, T. Thio, J. B. Pendry, and T. W. Ebbesen, "Theory of extraordinary optical transmission through subwavelength hole arrays," *Phys. Rev. Lett.*, vol. 86, no. 6, pp. 1114–1117, Feb. 2001.

[24] K. J. Klein Koerkamp, S. Enoch, F. B. Segerink, N. F. Van Hulst, and L. Kuipers, "Strong influence of hole shape on extraordinary transmission through periodic arrays of subwavelength holes," *Phys. Rev. Lett.*, vol. 92, no. 18, p. 183901, May 2004.

[25] C. Genet and T. W. Ebbesen, "Light in tiny holes," *Nature*, vol. 445, no. 7123, pp. 39–46, Jan. 2007.

[26] S. A. Maier, *Plasmonics: Fundamentals and Applications.* Berlin, Germany: Springer-Verlag, 2007.

[27] H. Raether, *Surface Plasmons on Smooth and Rough Surfaces an on Gratings.* Berlin, Germany: Springer-Verlag, 1986.